ACS APPLIED MATERIALS & INTERFACES

Research Article

www.acsami.org

Formation of An Ionic PTCA-β-CDNH$_2$ Complex and Its Application for Phenol Sensing in Aqueous Phase

Lingling Liu, Xiangli Chen, Kaiqiang Liu, Meixia He, Gang Wang, Xingmao Chang, and Yu Fang*

Key Laboratory of Applied Surface and Colloid Chemistry (Ministry of Education), School of Chemistry and Chemical Engineering, Shaanxi Normal University, Xi'an 710119, People's Republic of China

Supporting Information

ABSTRACT: On the basis of proton transfer in aqueous phase, we prepared a water-soluble and highly fluorescent ionic complex of 3,4,9,10-perylene tetracarboxylic acid (PTCA) and 6-deoxy-6-amino-β-CD (β-CDNH$_2$) and studied its fluorescence behavior. It was found that the fluorescence emission of the complex is sensitive and selective to the presence of trace amount of toxic phenolic compounds, in particular phenol, which is crucial for water quality control. The detection limit (DL) of the method to the analyte is ~0.03 μM, a lowest value reported in literatures for similar techniques. Interestingly, the detection at an unprecedented subnanogram (DL, ~0.12 ng/cm^2) level can also be conducted in a visualized manner, which may provide a simple and low-cost protocol for on-site and real-time detection of the analyte. Moreover, the complex is humidity sensitive in dry state, and its color changes from bright yellow to bright green when exposed to wet vapor. Unlike other PTCA bisimide derivatives, preparation of the ionic complex of PTCA/β-CDNH$_2$ is simple and avoids complicated synthetic burden. Furthermore, introduction of methanol into the aqueous solution of the complex resulted in aggregation as indicated by solution color change and proved by transmission electron microscopy and dynamic light scattering studies, which explains why the compound in dry state is sensitive to the presence of water and water vapor. X-ray diffraction, UV–vis, and fluorescence studies uncovered the H-packing nature of the structure of the aggregate.

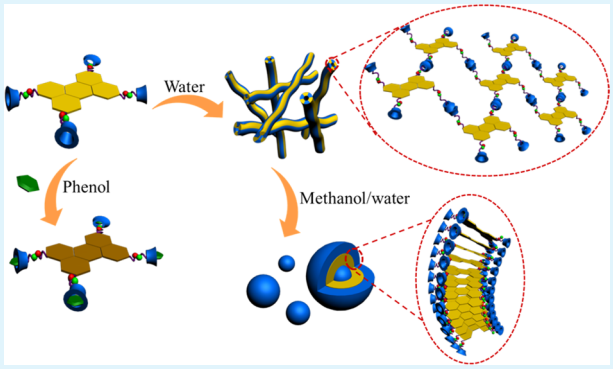

KEYWORDS: *3,4,9,10-perylene tetracarboxylic acid, 6-deoxy-6-amino-β-cyclodextrin, ionic complex, phenol, fluorescence*

1. INTRODUCTION

Derivatives of perylene-3,4,9,10-tetracarboxylic acid bisimides (PBIs) are a group of typical aromatic chromophores and have found a great variety of applications in different areas of organic photoelectronics and fluorescence chemical/biochemical sensors due to their exceptional optical and electronic properties, such as high fluorescence quantum yields, good photochemical and electrochemical stability, and great potential in derivatization.[1−8] The main drawback of PBI derivatives is their poor solubility in commonly found solvents. Therefore, substitution at the bay and imide positions has been used to improve their solubility and to tune their packing properties.[9−15]

The strategy, however, as mentioned for enhancing their solubility, is often inevitably realized via complicated organic synthesis, and thereby, it would be of interest if noncovalent interactions such as hydrogen bonding, $\pi-\pi$ stacking, van der Waals interaction, host−guest interaction, electrostatic interaction, and so on could be utilized to improve the water solubility of the derivatives, and realize their functions in aqueous phase.

Cyclodextrins (CDs) is a family of cyclic oligosaccharides that are composed of six to eight α-D-glucopyranoside units in a ring linked by α-1,4-glycosidic bonds. The CDs possess a hydrophilic exterior surface and hydrophobic interior cavity on the truncated cone. It is the cavity that makes CDs become a group of organic hosts for the inclusion of some organic molecules in aqueous phase.[16,17] In addition, the hydroxyl groups presenting at different positions can be selectively converted into other desired functional structures, and the derivatives as obtained may be further used for constructing diverse supramolecular architectures.[18−20]

The attractive advantages of CDs and those of PBI have inspired us to make a hypothesis that is combination of CDs and PBI via a noncovalent method would lead to weakening of the strong $\pi-\pi$ interaction between PBI units, resulting in increase in the water solubility of the chromophore which is the basis for being used in aqueous phase. Accordingly, a water-soluble complex of PBI and CDs was prepared by using perylene tetracarboxylic acid (PTCA) and 6-deoxy-6-amino-β-CD (β-CDNH$_2$) as the reactants (c.f. Scheme 1). Interestingly, PTCA/(β-CDNH$_2$)$_4$ was found to undergo a remarkable structural change in the presence of water that result in a

Received: July 5, 2015
Accepted: September 8, 2015
Published: September 8, 2015

DOI: 10.1021/acsami.5b06011
ACS Appl. Mater. Interfaces 2015, 7, 21364−21372

Scheme 1. Structure of PTCA/(β-CDNH$_2$)$_4$, Where the Conical Cartoon Stands for β-CD

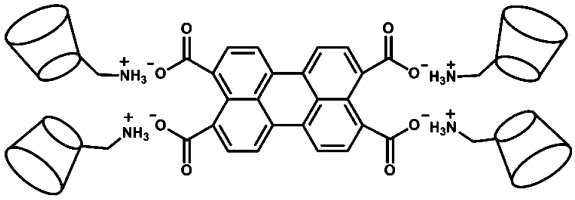

yellow-to-green color transition. Furthermore, introduction of β-CD makes the emission of the complex sensitive to the presence of phenol, a poisonous chemical commonly found in contaminated water, and the relevant test is fast and possesses a detection limit (DL) of ~0.03 μM. Moreover, the detection can also be conducted in a visualized way with a DL lower than 0.12 ng/cm^2, which is an unprecedented result reported until now. We report the details here.

2. EXPERIMENTAL SECTION

2.1. Materials. β-Cyclodextrin, *p*-toluenesulfonyl chloride (>98%) were purchased from Sigma-Aldrich. 3,4,9,10-Perylene tetracarboxylic dianhydride (>98%) was purchased from Tokyo Chemical Industry Co., Ltd. (TCI). KOH, ethanol, acetone, and hydrochloric acid were obtained from Sinopharm Chemical Reagent Co., Ltd., as analytical pure reagents. The chemicals, except those specially indicated, were used without further purification. Water used in this work was acquired from a Milli-Q reference system.

2.2. Measurements. ^{1}H NMR spectra were measured on Bruker AV 600 NMR spectrometers in DMSO-d_6 with tetramethylsilane (TMS) as an internal standard. Pressed KBr disks for the powder samples were used for the transmission infrared (FTIR) spectroscopy measurements, and their FTIR spectra were obtained with a Bio-Rad FTIR spectrometer. UV−vis absorption spectra of all samples were recorded on a spectrophotometer (Lambda 950, PerkinElmer, Waltham, MA). Mass spectrometry measurements were performed on an AXIMA-CFR in MALDI-TOF mode by using a-cyano-4-hydroxycinnamic acid (CCA) as the matrixes. TEM images were obtained using JEOL JEM-2100 transmission electron microscope at an acceleration voltage of 200 kV. DLS measurements were conducted on a Malvern Zeta Sizer Nano-ZS90. The XRD pattern of the sample was obtained by using a D/Max-2550/PC with Cu Kα X-ray radiation generated under a voltage of 40 kV and a current of 40 mA. The scan rate was 0.5° min^{-1} and the scan range of 2θ was from 1.5 to 10°. Fluorescence measurements were conducted with a time-correlated single photon counting Edinburgh Instruments FLS 920 fluorescence spectrometer at room temperature.

3. RESULTS AND DISCUSSION

3.1. Association between PTCA and β-CDNH$_2$. PTCA contains four hydrophilic carboxyl groups and exists as poly(carboxylic acid)s, but the strong $\pi-\pi$ stacking of the perylene unit still resists dissolving in water. To increase water solubility of the compound and get the desired PTCA/(β-CDNH$_2$)$_4$ complex, we introduced 4 equiv of β-CDNH$_2$ in order to make the carboxyl groups fully turned into carboxylates. As both carboxylic acids and the amine are weak, all the tests were conducted in pure water. The formation of the ionic complex was confirmed by several observations from multiple analytical techniques.

First, as observed in the experimental test, the addition of β-CDNH$_2$ to the PTCA solution resulted in rapid red to green color change, and instant and complete dissolution of the solid PTCA at the bottom of the reaction vessel (c.f. the inset of Figure 1) largely because of proton transfer from the carboxyl

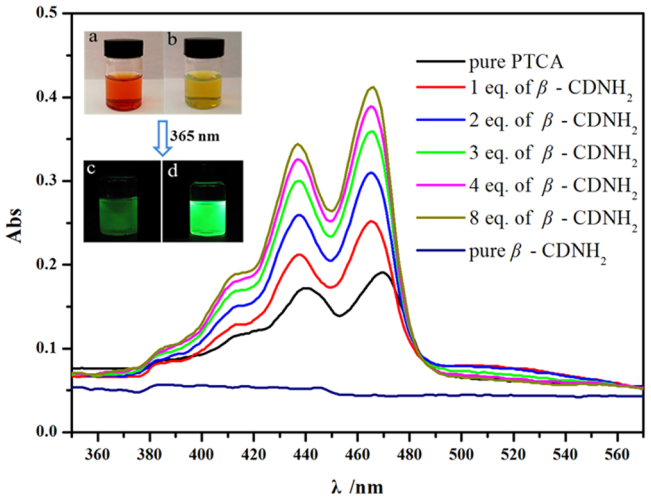

Figure 1. UV−vis absorption spectra of the aqueous solution of PTCA in the presence of different amount of β-CDNH$_2$, of which the concentration of PTCA is 5 × 10^{-6} M. (Inset) Photographs of the aqueous solutions of PTCA and PTCA/β-CDNH$_2$ (1:4 in molar ratio) under (a and b) daylight and (c and d) UV light (365 nm).

groups of PTCA to the amino group of β-CDNH$_2$, thus leading to the dissolution of PTCA and the dis-assembling of solubilized PTCA in solution. In other words, the perylene unit may exist in different states in the solution of pure PTCA and that of the complex of PTCA/β-CDNH$_2$, an indication of different electronic coupling of the π-system in the two states.[21]

Second, the interaction between the two components during mixing was monitored by UV−vis absorption spectroscopy measurement, and the results are shown in Figure 1. With reference to the figure, it is seen that PTCA showed three absorption bands positioning at 410, 440, and 471 nm, respectively. References to relevant literature,[8,11] it is no doubt that the peaks appearing at 410, 440, and 471 nm could be recognized as the excitation of the free state (monomer) of the chromophore, and the one around ~510 nm the absorption of the aggregated state of the chromophore. For β-CDNH$_2$, however, there is no obvious absorption within the wavelength range studied. Interestingly, the absorption bands of PTCA shifted from 440 and 471 nm to 437 and 464 nm, respectively, and the weakest one showed very little blue shift after the addition of β-CDNH$_2$, suggesting that the packing nature of the perylene units did not change during the test. Moreover, with increasing the molar ratio of β-CDNH$_2$ to PTCA, the intensity of the absorption gradually increased, which may be ascribed to the increase in the distance between the PTCA scaffolds. That is to say, the close $\pi-\pi$ aggregation may be weakened due to the bulky β-CDNH$_2$, which can suppress the electronic coupling of the PTCA aromatic rings in the H-aggregates. It is noteworthy that further addition of β-CDNH$_2$ after the ratio of it to PTCA reached 4:1 showed little effect upon the absorption of the solution as evidenced by the fact that the UV−vis spectrum of the system with an 8:1 ratio is almost the same to that with a ratio of 4:1, indicating the formation of a 4:1 complex of the two components.

Third, results from ^{1}H NMR titration tests are in support of the tentative conclusion. Reference to the spectra shown in Figure S1a reveals that with increasing the molar ratio of β-CDNH$_2$ to PTCA, the chemical shifts of a and b, which are two typical protons of the latter, increase gradually. Further analysis of the data demonstrates a clear 1:4 complex formation

DOI: 10.1021/acsami.5b06011
ACS Appl. Mater. Interfaces 2015, 7, 21364−21372

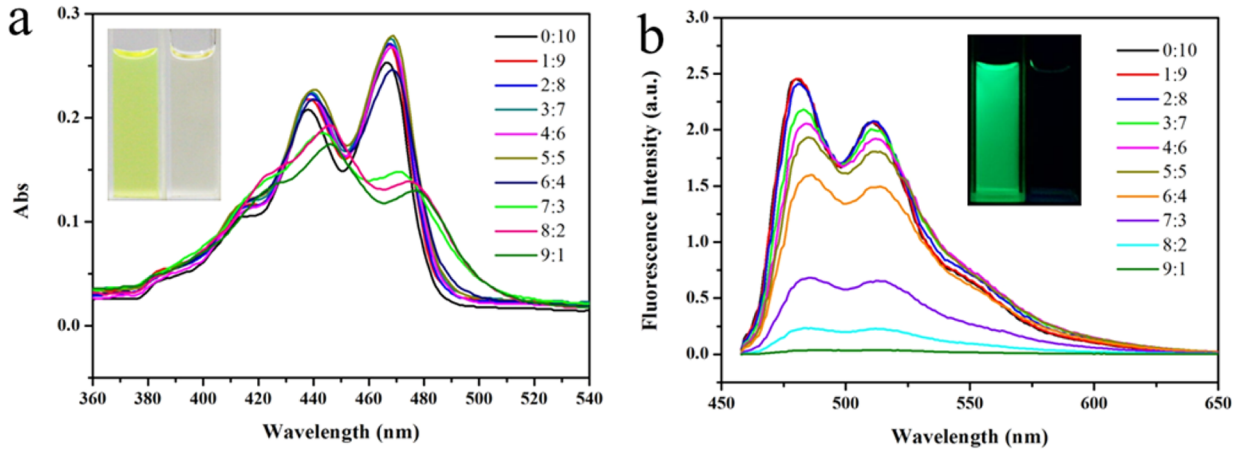

Figure 2. (a) Solvent-dependent UV−vis spectra and (b) fluorescent emission spectra of PTCA/(β-CDNH$_2$)$_4$ (5×10^{-6} M, λ_{ex} = 438 nm) in methanol/water binary solvents. The volume ratio shown in the inset is defined as methanol to water. The photographs of PTCA/(β-CDNH$_2$)$_4$ in (left) pure water and (right) methanol/water (9:1, v/v) (a) in sunlight and (b) upon irradiation at 365 nm.

between PTCA and β-CDNH$_2$, as seen in the plots depicted in Figure S1b.

Fourth, FT-IR measurements also confirm the formation of PTCA/(β-CDNH$_2$)$_4$ complex (c.f. Figure S2). Reference to the spectra reveals that the amide absorption band at 3014 cm^{-1} for pure β-CDNH$_2$ shifted to 2940 cm^{-1} after formation of the complex, which can be taken as a direct evidence of formation of $-NH_3^+$.[22,23] In addition, for PTCA/(β-CDNH$_2$)$_4$, a new absorption appeared at 1608 cm^{-1}, suggesting presence of $-COO^-$ in the complex, while the corresponding absorption of the carboxyl group in pure PTCA is at 1697 cm^{-1}. These results confirmed the ionic nature of the complex. Moreover, it is interesting to note that the stretching vibration of the perylene core in pure PTCA appeared at 1586 cm^{-1} but red-shifted to 1435 cm^{-1} upon association with β-CDNH$_2$, a result in support of the tentative conclusion described above.

Formation of PTCA/(β-CDNH$_2$)$_4$ was accompanied by increase in the fluorescence emission intensity of PTCA as evidenced by the ratio of β-CDNH$_2$ to PTCA dependent fluorescence spectra of the system shown in Figure S3 and the fluorescence picture depicted in the inset of Figure 1.

3.2. Aggregation of PTCA/(β-CDNH$_2$)$_4$. Benefiting from the introduction of β-CDNH$_2$, the complex exhibits favorable solubility in pure water in contrast to organic solvents, and thereby, introduction of organic solvents, such as methanol, into water may result in aggregation of the complex, which must be accompanied by changes in the optical properties of the systems. Accordingly, the UV−vis absorption spectra of the methanol−water mixture solutions of PTCA/(β-CDNH$_2$)$_4$ with different compositions of the binary solvents were measured, and the results are shown in Figure 2a. With reference to the figure, it is seen that the profile of the absorption spectrum of PTCA/(β-CDNH$_2$)$_4$ is largely dependent upon the composition of the solvents. The spectra are characterized by two sharp absorptions centering at 437 and 464 nm, respectively, when the volume fraction of methanol is less than 0.6, but further increase in the fraction of methanol resulted in a great change of the profile of the absorption as reflected by intensity decrease and intensity inversion of the two most intensive absorption bands. Another variation resulted from increasing methanol content is the broaden and blue-shift of the dominant absorption band of the complex, which should be results of strong electronic coupling with a H-stacking arrangement, in the binary solvents system in particular when methanol fraction exceeds a critical value.[1,11,24,25] Concomitantly, the solution color changed from green in pure water to light yellow in 9:1 methanol/water mixture (c.f. Figure 2a inset).

The aggregation of PTCA/(β-CDNH$_2$)$_4$ in the binary solvents was also monitored by fluorescence measurements, and the results are shown in Figure 2b. Clearly, the initial addition of methanol only resulted in a little bit decrease in the fluorescence emission, but a sharp transition was observed when the volume fraction of methanol in the mixture solvents exceeds 0.6, which is in accordance with that observed in UV−vis studies. The sharp intensity transition may be a sign of dense packing of the perylene unit, an equivalent of increase of concentration, due to inner filtering effect.[26] In other words, the complex should exist in less-aggregated state when the solvent is pure water or methanol−water mixtures provided the methanol fraction (v/v) is less than 0.6, indicating that introduction of the bulky β-CD and ionic structure is an effective strategy to screen $\pi-\pi$ stacking of the perylene units within the system and increase the solubility of the perylene derivative. As for why the addition of methanol enhances aggregation of the complex, it may be understood by considering its noncompatibility with the ionic structure of the complex and the highly hydrophilic nature of one of the two components, β-CD. It is the noncompatibility that makes the molecules of PTCA/(β-CDNH$_2$)$_4$ in the system get closer to each other, and result in strong $\pi-\pi$ stacking of the perylene units within the system, as shown by the change of the UV−vis absorptions (c.f. Figure 2a).

Two additional points need to be noted: (1) aggregation of the complex does not mean phase separation in a macroscopic scale, and (2) the profile of the fluorescence emission spectrum of the aggregate is almost independent of the solvent composition, that is no matter monomeric or aggregated state, the profile is almost the same, a property very different from other PBI derivatives.[27,28] A similar observation was also made in concentration-dependent studies of the fluorescence emission and absorption of the complex conducted in aqueous phase. The results are shown in Figure S4. As expected, higher concentration of the complex resulted in aggregation, typically in H-form.[8]

DOI: 10.1021/acsami.5b06011
ACS Appl. Mater. Interfaces 2015, 7, 21364−21372

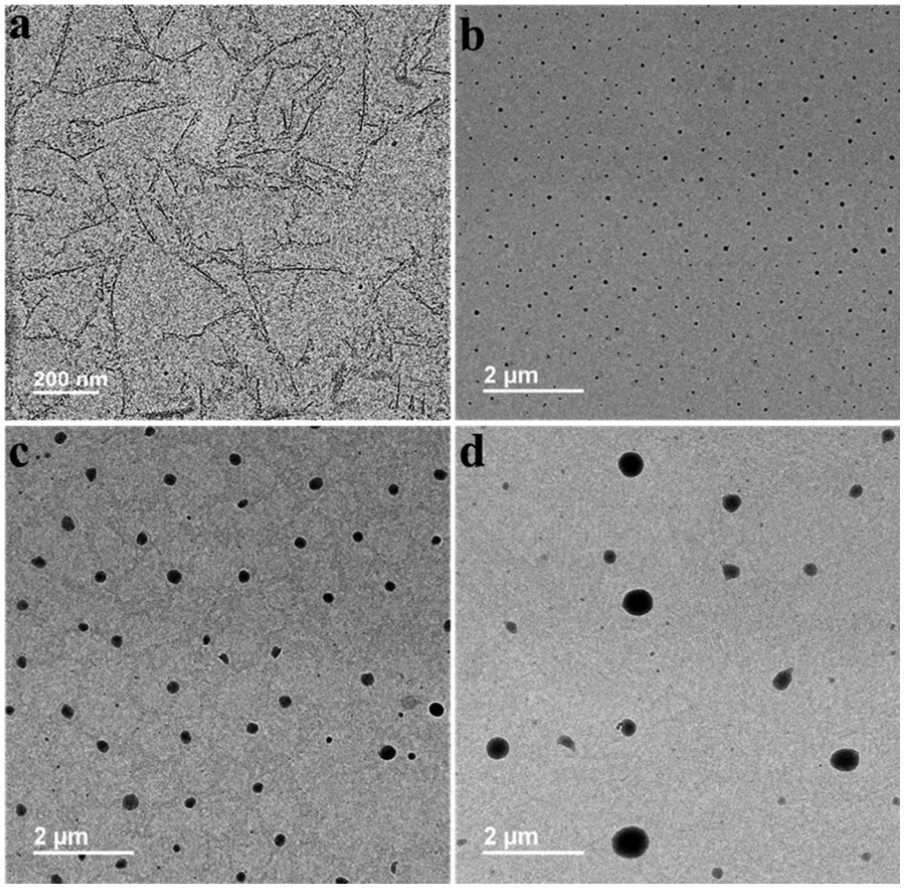

Figure 3. Solvent-dependent TEM images of the aggregate of PTCA/(β-CDNH$_2$)$_4$ (1×10^{-4} M) in different solvents: (a) water, (b) 7:3 methanol/water, (c) 8:2 methanol/water, and (d) 9:1 methanol/water.

Scheme 2. Assembly Models of PTCA/(β-CDNH$_2$)$_4$ in Water and Methanol/Water Mixed Solvents

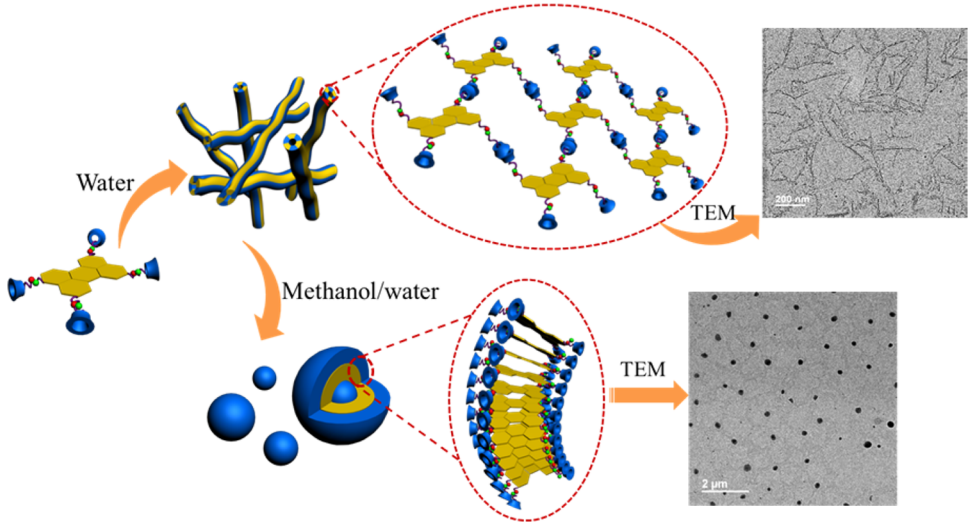

Morphology of the Aggregate of PTCA/(β-CDNH$_2$)$_4$. To obtain direct evidence of the aggregation of PTCA/(β-CDNH$_2$)$_4$, the microstructures of the aggregates of PTCA/(β-CDNH$_2$)$_4$ in methanol–water binary solvents of different compositions were examined. Figure 3 shows the TEM images of them obtained from 7:3, 8:2, and 9:1 of methanol–water mixtures with a concentration of 1×10^{-4} M. Reference to the images reveals that the aggregate morphology of the complex is strongly dependent upon the solvent composition. It is seen that initially the complex existed in loosely packed nanofibrous structures in pure water with an average length of 300 nm, and then changed into spherical structures with increasing the content of methanol. The average diameter of the aggregate increased along with increasing methanol content, and specifically, with the ratio of methanol to water increased from 7:3 to 8:2 and then to 9:1, the average diameter increased from 80 to 249 and then to 800 nm. This observation was

DOI: 10.1021/acsami.5b06011
ACS Appl. Mater. Interfaces 2015, 7, 21364–21372

further confirmed by the results from dynamic light scattering (DLS) studies (c.f. Figure S5).

Association with aforementioned spectrum changes and the natural hydrophilicity of PTCA/(β-CDNH$_2$)$_4$, it is reasonable to infer that the morphology of the aggregate should be mainly determined by the polarity of the solvent. For the formation of fibrous structure in pure water, a probable mechanism is that the perylene core of PTCA may stack in a parallel manner and form a fiber with the π-structure of PTCA in the core and the four β-CDNH$_2$ units pointing to different sides of the PTCA plane. With exception of $\pi-\pi$ stacking, another possible force for driving the fibrous structure formation may be hydrogen bonding between adjacent β-CD units (c.f. Scheme 2). XRD analysis, which will be presented latter, confirmed this tentative argument. For the systems of methanol contents of more than 0.7, the hydrophobic perylene core of the complex may adopt a face-to-face stack between adjacent PTCA units as revealed by UV−vis studies of the mixture solvents systems. However, with increasing methanol content, the β-CD units may point to the same side of the PTCA structure due to their hydrophilic nature, favoring the formation of spherical supramolecular architectures (c.f. Scheme 2).[27] The big difference in the particle size must be a result of increase in the number of the complex within an aggregate due to volume fraction increase of methanol in the binary solvents.

3.4. Hydrochromic Property of PTCA/(β-CDNH$_2$)$_4$. Inspired by the aforementioned morphology changes as a result of variation of the binary solvents composition, it is anticipated that change of PTCA/(β-CDNH$_2$)$_4$ from dry state to wet state may accompany a significant color change. In order to explore this speculation, the word "SNNU", which is the abbreviation of Shaanxi Normal University, the affiliation of the authors, was written on a filter paper by using a ball-pen, which was prefilled with the aqueous solution of PTCA/(β-CDNH$_2$)$_4$ (c.f. Figure 4). Initially, the word showed a very bright green

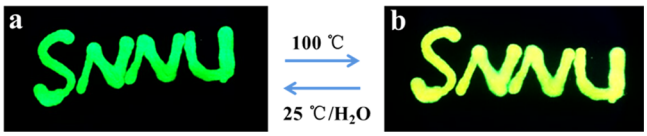

Figure 4. (a) Fluorescent photographs of handwriting with the aqueous solution of PTCA/(β-CDNH$_2$)$_4$ on a filter and (b) after drying at 100 °C.

color under UV light illumination (365 nm), but drying makes the color of the word change into yellow. The yellow color could be fully recovered by leaving the paper in a moist atmosphere. Moreover, the reversible color change can be repeated many times.

3.5. Nature of Hydrochromism. The hydrochromic behavior of the complex was further studied by measuring its UV−vis absorption spectra in different states, and the results are depicted in Figure S6a. It is clearly seen that a significant shift in the wavelength maximum from 447 to 473 nm takes place when the film is treated with water, of which a corresponding change in fluorescence emission spectrum was also observed (c.f. Figure S6b). The shift and change in the profile of the absorption and emission spectra demonstrated that wetting promotes dis-aggregation of the aggregated structure of the complex.

XRD study may help the understanding of the origin of the hydrochromic behavior of PTCA/(β-CDNH$_2$)$_4$.[29,30] Specifically, the XRD pattern of the initial yellow-colored PTCA/(β-CDNH$_2$)$_4$ film is characterized by six strong peaks appearing at 2θ = 6.31, 8.95, 10.80, 12.87, 17.22, and 18.82°, respectively (c.f. Figure S7), of which the corresponding d values are 1.399, 0.987, 0.818, 0.687, 0.514, and 0.471 nm, respectively, indicating highly ordered crystal-like structure of the aggregate. Upon hydration, the peaks shifted to 6.19, 8.75, 10.67, 12.50, 16.79 and 17.32°, respectively, and the d values were calculated to be 1.426, 1.009, 0.828, 0.707, 0.527, and 0.511 nm, respectively, suggesting swelling of the aggregate, which must be a result of water-promoted increase in the interplanar spacing and explain why the color of the aggregate of the complex changed from yellow-to-green after wetting. This feature may enable fabrication of a humidity sensing film by utilizing the fluorescent complex of PTCA/(β-CDNH$_2$)$_4$. Further analysis of the XRD data reveals that the ionic complex packed in a tetragonal mode because for both samples the spacings (the d values) follow the ratio of $1:(1/\sqrt{2}):(1/2):(1/\sqrt{5}):(1/\sqrt{8}):(1/3)$.

3.6. Phenol Sensing. To explore the possible application of PTCA/(β-CDNH$_2$)$_4$, we investigated phenol effect to the fluorescence emission of the complex in aqueous phase. This is because the benzene ring of the phenol is electron-rich due to electron donating property of the hydroxyl group, whereas the latter is electron-poor due to the electron withdrawing character of the carboxyl groups. It is the opposite property that may make PTCA/(β-CDNH$_2$)$_4$ possess specific affinity to phenol. Another possible affinity of the complex may come from host−guest interaction between β-CD and phenol.[31,32] Affinity of the analyte to the complex, no matter which mechanism it follows, must be favorable for the possible sensing.

As it is known, phenol is important due to its widespread uses in the production of polycarbonates, epoxies, Bakelite, nylon, detergents, herbicides, and numerous pharmaceutical drugs.[33−36] However, phenol is also listed as a high-priority pollutant by the U.S. Environmental Protection Agency and other organizations because of its high toxicity even at a very low concentration.[37,38] Therefore, sensitive and selective detection of phenol in water is of great importance. In fact, gas chromatography, liquid chromatography, UV spectroscopy, colorimetry, and varies electrochemical methods have been used for the detection.[39−46] Utilization of the techniques, however, usually requires sophisticated instrumentation, multistep procedures, slow catalytic kinetics, poor stability, specific enzymes, and so on, and these shortcomings make them less convenient for rapid and on-site detection. Accordingly, phenol effect to the fluorescence emission of the complex in aqueous phase was studied and the results are depicted in Figure 5. It is seen that introduction of phenol induces remarkable reduction of the fluorescence emission. As a control, phenol could not quench the fluorescence emission of pure PTCA (c.f. the inset of Figure 5), indicating the importance of β-CDNH$_2$ and suggesting, indirectly, that the approach of phenol to the fluorescent complex, which is a prerequirement for the fluorescence quenching, may be realized through the host−guest interaction between them. This tentative explanation was further confirmed by the latter ^{1}H NMR studies. Further inspection of the inset of Figure 5, which is the Stern−Volmer plots of the data from the studies, reveals that for the system of the ionic complex and within the whole concentration range studied the plot is close to linear, suggesting the homogeneity of the environment of the complex. This result is not difficult to

DOI: 10.1021/acsami.5b06011
ACS Appl. Mater. Interfaces 2015, 7, 21364−21372

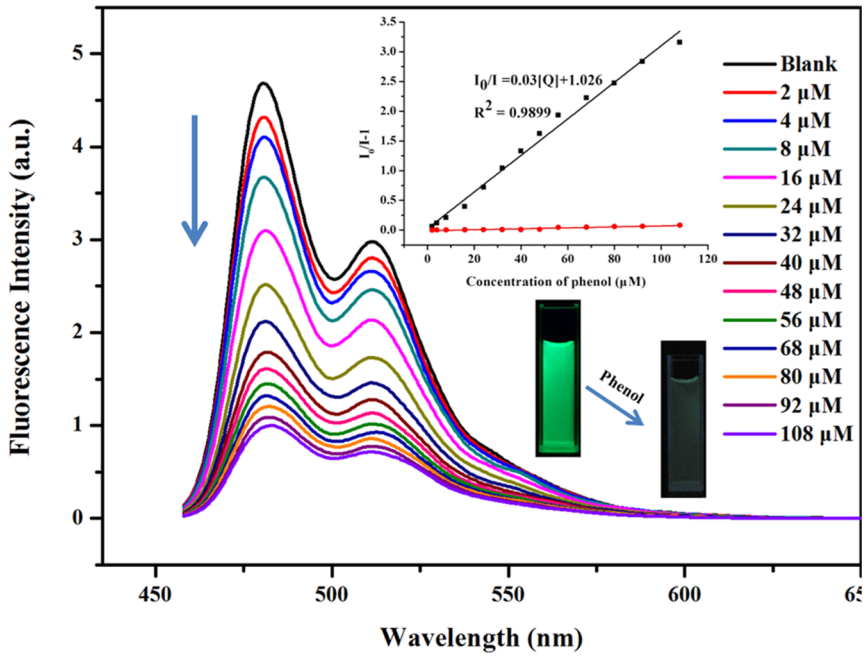

Figure 5. Fluorescence emission spectra of the aqueous solution of PTCA/(β-CDNH$_2$)$_4$ (2×10^{-6} M) in the presence of different concentrations of phenol. (Inset) Corresponding (black) Stern–Volmer plot of the quenching data and (red) a plot from a reference system, of which the only difference is that PTCA was adopted instead of the complex. (Inset) Photographs of (left) PTCA/(β-CDNH$_2$)$_4$ and (right) PTCA/(β-CDNH$_2$)$_4$+Phenol (data error: ± 3%).

Table 1. Key Parameters of Different Methods for Phenol Detection

method		medium	response time	detection limit (M)	ref
electrochemistry	Tyr-based detection	PBS buffer	10 min	10^{-9}–10^{-3}	44
		PBS buffer	10 min	5×10^{-8}	46
	electrocatalytic oxidation	PBS buffer	3 s	5×10^{-7}	43
chromatography	liquid chromatography	water	5 min	3×10^{-8}	40
	gas chromatography	water	7.24 min	2×10^{-8}	39
spectrophotometry	UV–vis spectrophotometry	water		10^{-6}	42
	4-aminoantipyrine (4-AAP)	PBS buffer		4×10^{-6}	41
fluorescence spectrophotometry		water		8×10^{-3}	16
		water		10^{-2}	17
		water	instantaneous	3×10^{-8}	this work
visualization		water	instantaneous	0.12 ng/cm^2	this work

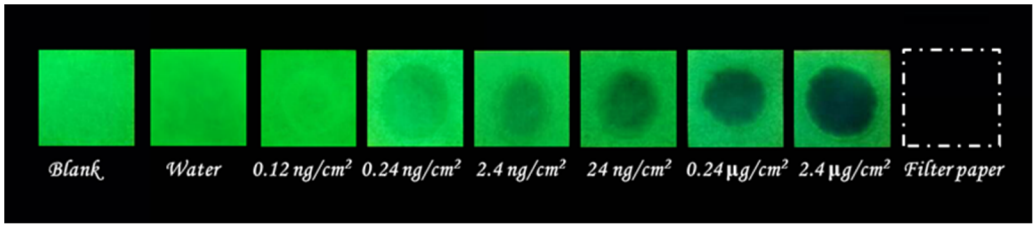

Figure 6. Photographs of the PTCA/(β-CDNH$_2$)$_4$ pretreated filter papers (20 μL, 2.5×10^{-4} M for each) in the presence of different amount of phenol (10 μL) of which the concentration of phenol increases from left to right (0, 0, 5×10^{-8}, 1×10^{-7}, 1×10^{-6}, 1×10^{-5}, 1×10^{-4}, and 1×10^{-3} M) when viewed under 365 nm UV illumination. The diameter of each spot is ~0.7 cm,

understand due to excellent solubility of the complex in water. Further inspection of the plot reveals that trace amount of phenol in aqueous phase could cause noteworthy reduction of the fluorescence emission. For example, 2 μM of the analyte induced more than 7% fluorescence quenching. The linear range could be from 0 to 108 μM, enabling quantitative detection of phenol. The calculated detection limit (DL) of the method as established is about 0.03 μM, of which the details of the calculation are provided in the Supporting Information. To our knowledge, this is the best result for fluorescence detection of phenol reported in literatures, not to mention the medium used in the present work is just pure water (c.f. Table 1).

Detection of phenol can be also conducted in a visualized way. In the detection, a test paper was prepared by simply treating a piece of ordinary filter paper (~1 × 1 cm) with 20 μL of an aqueous solution of the ionic complex (2.5×10^{-4} M).

DOI: 10.1021/acsami.5b06011
ACS Appl. Mater. Interfaces 2015, 7, 21364–21372

Scheme 3. Schematic Illustration of the Mechanism for Sensing Phenol

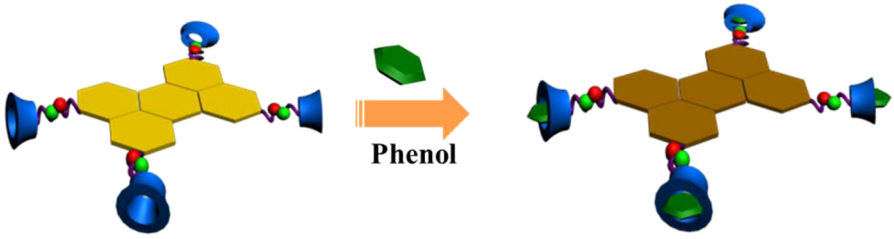

The test can be conducted after drying the paper in air at room temperature. In a typical test, 10 μL of an aqueous solution of phenol of different concentrations was added on the surface of the paper. Naked-eye observation under UV light illumination can tell if there is any phenol in the solution under test. Figure 6 shows some of the results. The detection is instantaneous and the DL of the test is lower than 0.12 ng/cm^2, which is an unprecedented result.

Considering the complexity of the composition of contaminated water, it should be of interest to check if the fluorescence emission of PTCA/(β-CDNH$_2$)$_4$ is sensitive to the presence of other commonly found organic contaminates. The results are shown in Figure S8. It is seen that the presence of amines, such as propylamine, ethylenediamine, triethylamine, methylamine, ammonia and hydrazine hydrate, and so on, enhances the emission of the complex in aqueous phase. As for organic solvents, such as chloroform, benzene, toluene, dichloromethane, THF, and acetone, as well as *N*,*N*-dimethylaniline, aniline, they showed little effect on the emission. With regard to *p*-nitrophenol, a derivative of phenol, it also showed a certain degree of quenching to the fluorescence emission of the system, but the efficiency is significantly lower than that of phenol. This result may be understood by considering its larger water solubility and lower electron-density on the benzene ring if compared with that of phenol. Clearly, both factors go against its inclusion by the host, showing lower quenching efficiency. In addition, lower electron density is also unfavorable for its sensing. The higher sensitivity of the complex to phenol can be attributed to the inclusion of the analyte by the β-CD cavity as confirmed by the ^{1}H NMR spectroscopy result of PTCA/(β-CDNH$_2$)$_4$ in the presence of phenol (c.f. Figure S9a).

With reference to the ^{1}H NMR spectra, it is clearly seen that the signals of the protons of a, b and c on phenol ring shifted to higher field if compared with pure phenol, suggesting inclusion of phenol within the cavity of β-CD.[47] To further confirm if phenol is really hosted within the cavity of β-CD, an additional experiment was conducted. Considering the fact that the internal polarity of β-CD, which is about 1.47,[48] is close to that of cyclohexane, the ^{1}H NMR spectrum of phenol in deuterated cyclohexane was recorded and the result is depicted in Figure S9b. From the figure, it is found that the signals of the protons of a, b, and c on phenol ring also shifted to higher field, which is in accordance with the results of presence of PTCA/(β-CDNH$_2$)$_4$. Beasides, the 2D NOESY NMR spectrum of PTCA/(β-CDNH$_2$)$_4$ with phenol is given in Figure S10. The protons of the inner cavity of β-CD were correlated to the phenol protons, an indication of complexation between β-CD and phenol. Clearly, these results further supports the possible sensing mechanism proposed for explanation of the test as shown in Scheme 3

To further understand the mechanism of the quenching process, we conducted fluorescence lifetime measurements, and the results are shown in Figure S11. It is seen that the intensity-based plot is a straight line, while the lifetime-based one is a line with a slop of nearly zero, suggesting that the quenching is dominated by formation of a non/weak-fluorescent complex, PTCA/(β-CDNH$_2$)$_4$-phenol, a typical static quenching process. These results explain why the fluorescence emission of the complex is sensitive to the presence of the analyte.

4. CONCLUSIONS

In conclusion, a water-soluble, highly fluorescent complex was created via proton transfer from PTCA to β-CDNH$_2$ in aqueous phase. The ionic complex as produced shows a dramatic yellow to green color change upon wetting, a property not reported before for other water-soluble PBI derivatives. Moreover, the presence of β-CD in the complex makes its fluorescence emission sensitive to the presence of phenol in aqueous phase. The DL of the detection is about 0.03 μM. The presence of other commonly found chemicals and solvents shows little effect upon the detection. Moreover, the detection can be also conducted in a visualized way, and the DL could be lower than 0.12 ng/cm^2, a lowest result reported until now. The extraordinary performance of the complex in sensing has been partially ascribed to its affinity to the analyte due to host−guest interaction between β-CD and phenol. Considering the simple preparation, the ease of operation, and excellent performance, it may be concluded that the ionic complex as produced has a great potential to be used as a sensing reagent for phenol detection in aqueous phase. In addition, the research conducted in the present work may open up a new avenue for improving the water solubility of PBI derivatives via a noncovalent modification method.

■ ASSOCIATED CONTENT

Supporting Information

The Supporting Information is available free of charge on the ACS Publications website at DOI: 10.1021/acsami.5b06011.

Detailed experimental methods, determination limit, and supplementary figures and schemes. (PDF)

■ AUTHOR INFORMATION

Corresponding Author

*E-mail: yfang@snnu.edu.cn. Tel: 0086-29-81530786. Fax: 0086-29-81530787.

Notes

The authors declare no competing financial interest.

■ ACKNOWLEDGMENTS

We gratefully acknowledge financial support from the Natural Science Foundation of China (21273141, 21473110, and

DOI: 10.1021/acsami.5b06011
ACS Appl. Mater. Interfaces 2015, 7, 21364−21372

21527802), the 111 Project and the Program for Changjiang Scholars and Innovative Research Team in University of China (IRT1070).

REFERENCES

(1) Würthner, F. Perylene Bisimide Dyes as Versatile Building Blocks for Functional Supramolecular Architectures. *Chem. Commun.* **2004**, 1564−1579.
(2) Wasielewski, M. R. Self-Assembly Strategies for Integrating Light Harvesting and Charge Separation in Artificial Photosynthetic Systems. *Acc. Chem. Res.* **2009**, *42*, 1910−1921.
(3) Zang, L.; Che, Y.; Moore, J. S. One-Dimensional Self-Assembly of Planar π-Conjugated Molecules: Adaptable Building Blocks for Organic Nanodevices. *Acc. Chem. Res.* **2008**, *41*, 1596−1608.
(4) Che, Y.; Yang, X. M.; Liu, G. L.; Yu, C.; Ji, H. W.; Zuo, J. M.; Zhao, J. C.; Zang, L. Ultrathin n-Type Organic Nanoribbons with High Photoconductivity and Application in Optoelectronic Vapor Sensing of Explosives. *J. Am. Chem. Soc.* **2010**, *132*, 5743−5750.
(5) Ehli, C.; Oelsner, C.; Guldi, D. M.; Mateo-Alonso, A.; Prato, M.; Schmidt, C.; Backes, C.; Hauke, F.; Hirsch, A. Manipulating Single-Wall Carbon Nanotubes by Chemical Doping and Charge Transfer with Perylene Dyes. *Nat. Chem.* **2009**, *1*, 243−249.
(6) Wang, G.; Chang, X. M.; Peng, J. X.; Liu, K. Q.; Zhao, K. R.; Yu, C. M.; Fang, Y. Towards a New FRET System via Combination of Pyrene and Perylene Bisimide: Synthesis, Self-Assembly and Fluorescence Behavior. *Phys. Chem. Chem. Phys.* **2015**, *17*, 5441−5449.
(7) Jiang, W.; Li, Y.; Wang, Z. H. Tailor-Made Rylene Arrays for High Performance n−Channel Semiconductors. *Acc. Chem. Res.* **2014**, *47*, 3135−3147.
(8) Liu, Y.; Wang, K.-R.; Guo, D.-S.; Jiang, B.-P. Supramolecular Assembly of Perylene Bisimide with β-Cyclodextrin Grafts as a Solid-State Fluorescence Sensor for Vapor Detection. *Adv. Funct. Mater.* **2009**, *19*, 2230−2235.
(9) Kaiser, T.; Wang, H.; Stepanenko, V.; Würthner, F. Supramolecular Construction of Fluorescent J-Aggregates Based on Hydrogen-Bonded Perylene Dyes. *Angew. Chem., Int. Ed.* **2007**, *46*, 5541−5544.
(10) Backes, C.; Schmidt, C. D.; Hauke, F.; Bötcher, C.; Hirsch, A. High Population of Individualized SWCNTs through the Adsorption of Water-Soluble Perylenes. *J. Am. Chem. Soc.* **2009**, *131*, 2172−2184.
(11) Görl, D.; Zhang, X.; Würthner, F. Molecular Assemblies of Perylene Bisimide Dyes in Water. *Angew. Chem., Int. Ed.* **2012**, *51*, 6328−6348.
(12) Yang, S. K.; Shi, X. H.; Park, S.; Doganay, S.; Ha, T.; Zimmerman, S. C. Monovalent, Clickable, Uncharged, Water-Soluble Perylenediimide-Cored Dendrimers for Target-Specific Fluorescent Biolabeling. *J. Am. Chem. Soc.* **2011**, *133*, 9964−9967.
(13) Qu, J. Q.; Kohl, C.; Pottek, M.; Müllen, K. Ionic Perylenetetracarboxdiimides: Highly Fluorescent and Water-Soluble Dyes for Biolabeling. *Angew. Chem., Int. Ed.* **2004**, *43*, 1528−1531.
(14) Tang, T. J.; Herrmann, A.; Peneva, K.; Müllen, K.; Webber, S. E. Energy Transfer in Molecular Layer-by-Layer Films of Water-Soluble Perylene Diimides. *Langmuir* **2007**, *23*, 4623−4628.
(15) Gao, B. X.; Li, H. X.; Liu, H. M.; Zhang, L. C.; Bai, Q. Q.; Ba, X. W. Water-Soluble and Fluorescent Dendritic Perylene Bisimides for Live-Cell Imaging. *Chem. Commun.* **2011**, *47*, 3894−3896.
(16) Surpateanu, G. G.; Becuwe, M.; Lungu, N. C.; Dron, P. I.; Fourmentin, S.; Landy, D.; Surpateanu, G. Photochemical Behaviour upon the Inclusion for Some Volatile Organic Compounds in New Fluorescent Indolizine β-Cyclodextrin Sensors. *J. J. Photochem. Photobiol., A* **2007**, *185*, 312−320.
(17) Becuwe, M.; Landy, D.; Delattre, F.; Cazier, F.; Fourmentin, S. Fluorescent Indolizine-β-Cyclodextrin Derivatives for the Detection of Volatile Organic Compounds. *Sensors* **2008**, *8*, 3689−3705.
(18) Khan, A. R.; Forgo, P.; Stine, K. J.; D'Souza, V. T. Methods for Selective Modifications of Cyclodextrins. *Chem. Rev.* **1998**, *98*, 1977−1996.
(19) Chen, Y.; Liu, Y. Cyclodextrin-Based Bioactive Supramolecular Assemblies. *Chem. Soc. Rev.* **2010**, *39*, 495−505.
(20) Harada, A.; Takashima, Y.; Nakahata, M. Supramolecular Polymeric Materials via Cyclodextrin-Guest Interactions. *Acc. Chem. Res.* **2014**, *47*, 2017−2025.
(21) Liu, K.; Yao, Y. X.; Kang, Y. T.; Liu, Y.; Han, Y. C.; Wang, Y. L.; Li, Z. B.; Zhang, X. A Supramolecular Approach to Fabricate Highly Emissive Smart Materials. *Sci. Rep.* **2013**, *3*, 2372−2378.
(22) Kaleeswaran, D.; Vishnoi, P.; Murugavel, R. [3 + 3] Imine and β-ketoenamine tethered fluorescent covalent-organic frameworks for CO_2 uptake and nitroaromatic sensing. *J. Mater. Chem. C* **2015**, *3*, 7159−7171.
(23) Wei, H.; Chai, S. Z.; Hu, N. T.; Yang, Z.; Wei, L. M.; Wang, L. The microwave- assisted solvothermal synthesis of a crystalline two-dimensional covalent organic framework with high CO_2 capacity. *Chem. Commun.* **2015**, *51*, 12178−12181.
(24) Seibt, J.; Winkler, T.; Renziehausen, K.; Dehm, V.; Würthner, F.; Meyer, H.-D.; Engel, V. Vibronic Transitions and Quantum Dynamics in Molecular Oligomers: A Theoretical Analysis with an Application to Aggregates of Perylene Bisimides. *J. Phys. Chem. A* **2009**, *113*, 13475−13482.
(25) Chen, Q.; Blanchard, G. J. Orientational and Vibrational Relaxation Dynamics of Perylene in the Cyclohexane-Ethanol Binary Solvent System. *J. Phys. Chem. B* **2014**, *118*, 10525−10533.
(26) Zhang, J.; Wang, L. H.; Zhang, H.; Boey, F.; Song, S. P.; Fan, C. H. Aptamer-Based Multicolor Fluorescent Gold Nanoprobes for Multiplex Detection in Homogeneous Solution. *Small* **2010**, *6*, 201−204.
(27) Jiang, B. P.; Guo, D. S.; Liu, Y. Self-Assembly of Amphiphilic Perylene- Cyclodextrin Conjugate and Vapor Sensing for Organic Amines. *J. Org. Chem.* **2010**, *75*, 7258−7264.
(28) Balakrishnan, K.; Datar, A.; Naddo, T.; Huang, J. L.; Oitker, R.; Yen, M.; Zhao, J. C.; Zang, L. Effect of Side-Chain Substituents on Self-Assembly of Perylene Diimide Molecules: Morphology Control. *J. Am. Chem. Soc.* **2006**, *128*, 7390−7398.
(29) Lee, J.; Pyo, M.; Lee, S.-H.; Kim, J.; Ra, M.; Kim, W.-Y.; Park, B. J.; Lee, C. W.; Kim, J.-M. Hydrochromic Conjugated Polymers for Human Sweat Pore Mapping. *Nat. Commun.* **2014**, *5*, 3736−3746.
(30) Dalapati, S.; Addicoat, M.; Jin, S. B.; Sakurai, T.; Gao, J.; Xu, H.; Irle, S.; Seki, S.; Jiang, D. L. Rational design of crystalline supermicroporous covalent organic frameworks with triangular topologies. *Nat. Commun.* **2015**, *6*, 7786−7794.
(31) Chen, Q. C.; Zhang, R.; Wang, J.; Li, L.; Guo, X. H. Spherical Particles of α-, β- and γ-Cyclodextrin Polymers and Their Capability for Phenol Removal. *Mater. Lett.* **2012**, *79*, 156−158.
(32) Han, J. X.; Xie, K. J.; Du, Z. J.; Zou, W.; Zhang, C. β-Cyclodextrin Functionalized Polystyrene Porous Monoliths for Separating Phenol from Wastewater. *Carbohydr. Polym.* **2015**, *120*, 85−91.
(33) Tejado, A.; Pena, C.; Labidi, J.; Echeverria, J. M.; Mondragon, I. Physico-Chemical Characterization of Lignins from Different Sources for Use in Phenol- Formaldehyde Resin Synthesis. *Bioresour. Technol.* **2007**, *98*, 1655−1663.
(34) Hess, B.; van der Vegt, N. F. A. Predictive Modeling of Phenol Chemical Potentials in Molten Bisphenol A-Polycarbonate over a Broad Temperature Range. *Macromolecules* **2008**, *41*, 7281−7283.
(35) Yadav, G. D.; Salgaonkar, S. S. Loss Prevention and Waste Minimization with Cascade-Engineered Green Synthesis of Bisphenol-A from Cumene Hydroperoxide and Phenol using Heteropoly Acid-Supported Clay Catalysts. *Org. Process Res. Dev.* **2009**, *13*, 501−509.
(36) Wood, K. M. The Use of Phenol as a Neurolytic Agent: A Review. *Pain* **1978**, *5*, 205−229.
(37) Ahmaruzzaman, M.; Gayatri, S. L. Activated Tea Waste as a Potential Low-Cost Adsorbent for the Removal of *p*-Nitrophenol from Wastewater. *J. Chem. Eng. Data* **2010**, *55*, 4614−4623.
(38) Herterich, R. Gas Chromatographic Determination of Nitrophenols in Atmospheric Liquid Water and Airborne Particulates. *J. Chromatogr. A* **1991**, *549*, 313−324.

DOI: 10.1021/acsami.5b06011
ACS Appl. Mater. Interfaces 2015, 7, 21364−21372

(39) Meng, J. R.; Shi, C. Y.; Wei, B. W.; Yu, W. J.; Deng, C. H.; Zhang, X. M. Preparation of Fe_3O_4@C@PANI Magnetic Microspheres for the Extraction and Analysis of Phenolic Compounds in Water Samples by Gas Chromatography-Mass Spectrometry. *J. Chromatogr. A* **2011**, *1218*, 2841−2847.
(40) Huang, X. J.; Qiu, N. N.; Yuan, D. X. Direct Enrichment of Phenols in Lake and Sea Water by Stir Bar Sorptive Extraction Based on Poly(vinylpyridine-ethylene dimethacrylate) Monolithic Material and Liquid Chromatographic Analysis. *J. Chromatogr. A* **2008**, *1194*, 134−138.
(41) Zhu, L.; Gong, L.; Zhang, Y. F.; Wang, R.; Ge, J.; Liu, Z.; Zare, R. N. Rapid Detection of Phenol Using a Membrane Containing Laccase Nanoflowers. *Chem. - Asian J.* **2013**, *8*, 2358−2360.
(42) Lin, Z.; Xiao, Y.; Yin, Y. Q.; Hu, W. L.; Liu, W.; Yang, H. H. Facile Synthesis of Enzyme-Inorganic Hybrid Nanoflowers and Its Application as a Colorimetric Platform for Visual Detection of Hydrogen Peroxide and Phenol. *ACS Appl. Mater. Interfaces* **2014**, *6*, 10775−10782.
(43) Yang, C.-Y.; Chen, S.-M.; Tsai, T.-H.; Unnikrishnan, B. Poly(Diphenylamine) with Multi-Walled Carbon Nanotube Composite Film Modified Electrode for the Determination of Phenol. *Int. J. Electrochem. Sci.* **2012**, *7*, 12796−12807.
(44) Noh, S.; Yang, H. Sensitive Phenol Detection Using Tyrosinase-Based Phenol Oxidation Combined with Redox Cycling of Catechol. *Electroanalysis* **2014**, *26*, 2727−2731.
(45) Çevik, E.; Şenel, M.; Baykal, A.; Abasıyanık, M. F. A Novel Amperometric Phenol Biosensor Based on Immobilized HRP on Poly(glycidylmethacrylate)-Grafted Iron Oxide Nanoparticles for the Determination of Phenol Derivatives. *Sens. Actuators, B* **2012**, *173*, 396−405.
(46) Liu, F.; Piao, Y. X.; Choi, J. S.; Seo, T. S. Three-Dimensional Graphene Micropillar Based Electrochemical Sensor for Phenol Detection. *Biosens. Bioelectron.* **2013**, *50*, 387−392.
(47) Jiang, H. M.; Sun, H. J.; Zhang, S. B.; Hua, R. N.; Xu, Y. M.; Jin, S. B.; Gong, H. Y.; Li, L. NMR Investigations of Inclusion Complexes between β-Cyclodextrin and Naphthalene/Anthraquinone Derivatives. *J. Inclusion Phenom. Mol. Recognit. Chem.* **2007**, *58*, 133−138.
(48) Nakajima, A. A Study on the System of pyrene and β-Cyclodextrin in Aqueous Solution Utilizing the Intensity Enhancement Phenomenon. *Spectrochim. Acta* **1983**, *39A*, 913−915.

DOI: 10.1021/acsami.5b06011
ACS Appl. Mater. Interfaces 2015, 7, 21364−21372